Research Article

Dilshat U. Tulyaganov, Avzal Akbarov, Nigora Ziyadullaeva, Bekhzod Khabilov, and Francesco Baino*

Injectable bioactive glass-based pastes for potential use in bone tissue repair

https://doi.org/10.1515/bglass-2020-0003
Received Jun 25, 2020; revised Aug 08, 2020; accepted Sep 03, 2020

Abstract: In this study, injectable pastes based on a clinically-tested bioactive glass and glycerol (used as organic carrier) were produced and characterized for further application in regenerative medicine. The paste preparation route, apatite-forming ability in simulated body fluid (SBF) solution, viscoelastic behavior and structural features revealed by means of scanning electron microscopy (SEM), FTIR and Raman spectroscopy were presented and discussed, also on the basis of the major experimental data obtained in previous studies. A mechanism illustrating the chemical interaction between bioactive glass and glycerol was proposed to support the bioactivity mechanism of injectable pastes. Then, the results of *In vivo* tests, conducted through injecting moldable paste into osseous defects made in rabbit's femur, were reported. Animal studies revealed good osteoconductivity and bone bonding that occurred initially at the interface between the glass and the host bone, and further supported the suitability of these bioactive glass pastes in bone regenerative medicine.

Keywords: bioactive glass; injectable biomaterial; bioactivity; bone

1 Introduction

Glasses are definitely the most universal and essential materials made by humankind since the early stages of civilization. Nowadays, due to advancement acquired in the field of glass science, these materials have found applications in various technological domains, thus improving the quality of human life. Over the years, a wide range of glass compositions which belong to biomaterials category have been used in human biomedicine, greatly contributing to healthcare [1–5]. In particular, the original 45S5 Bioglass® invented by L. Hench in late 1960s [3, 4] (chemical composition (wt.%): 45 SiO_2, 24.5 CaO, 24.5 Na_2O, and 6.0) was successfully exploited for bone regeneration in more than 1.5 million patients [1].

In order to optimize the body's response according to the specific clinical applications, the first 45S5 Bioglass® and other types of bioactive glasses/glass-ceramics were initially used in the form of small cast solid pieces mainly for (a) treating conductive hearing losses in middle ear surgery and (b) replacement of tooth roots after being inserted into fresh tooth extraction sites in dentistry [6]. At present, the most common applications of bioactive glasses in the form of inorganic silica-based melt-derived compositions are based on particulates mainly as bone graft substitute in dentistry and orthopedics [7–10]. Thus, the first commercially developed 45S5 Bioglass® particulate (particle size 90–710 μm) under the trade name of PerioGlas® was applied for repairing interproximal bone defects in dentistry [9–12]. NovaBone® is another trade name of 45S5 Bioglass® particulate used in bone and tissue regeneration for over 20 years [6]. Furthermore, Biogran® is a restorable material that has the same composition of 45S5 glass particulates with size distribution in the range of 300–360 μm and was found to be effective in treatment periodontal defects and extraction sites [6, 13, 14].

To date, numerous clinical studies evidenced that commercial 45S5 glass-based products demonstrate a better treatment approach than conventional methods [14–22], although results of those clinical trials suggest that evaluated materials induced a "repair" response rather than a true regenerative response [15, 23]. Moreover, Profeta *et al.* [15] concluded that, due to their granular nature, 45S5 glass-based products cannot serve reliably as space-making materials in sites where there was no support for

***Corresponding Author: Francesco Baino:** Department of Applied Science and Technology, Politecnico di Torino, Turin, Italy; Email: francesco.baino@polito.it
Dilshat U. Tulyaganov: Department of Natural-Mathematical Sciences, Turin Polytechnic University in Tashkent, Tashkent, Uzbekistan
Avzal Akbarov, Nigora Ziyadullaeva, Bekhzod Khabilov: Department of Prosthodontics Tashkent State Dental Institute, Tashkent, Uzbekistan

a membrane while the soft tissue cover may cause its collapse during healing.

Recently, the latest evolution of bone graft material NovaBone® Dental Putty appeared on the market in the form of a pre-mixed composite of 45S5 Bioglass® particulate and a synthetic, absorbable binder that requires no special mixing procedures prior to use [1]. This new bone replacement product allowed meeting the important requirement of easy handling since normally surgeons tended to mix glass particles with blood from the patient to get putty-like composition which was pressed into the osseous defect [6, 9, 12].

In the last few years, the low-sodium fluoride-containing bioactive glass BG1d-BG (composition in wt%: 46.1 SiO_2, 28.7 CaO, 8.8 MgO, 6.2 P_2O_5, 5.7 CaF_2, 4.5 Na_2O) was found to be biocompatible not only upon implantation into rabbit femurs, but also when used for the treatment of jawbone defects in 45 human patients [24]. Recently, BG1d-BG was compared to the 45S5 Bioglass® to assess its effect on cell viability, proliferation and osteogenic differentiation of human mesenchymal stem cells (MSCs) in indirect and direct culture settings [25]. Results of this study indicated an advantage of BG1d-BG in regard to cell viability and proliferation due to combined effect of the lower amount of Na ions and the presence of Mg ions. Furthermore, in the direct culture setting the release of Ca ions appeared to be higher in the BG1d-BG group compared to 45S5 glass, which might explain its higher stimulatory effect on cell viability and proliferation [25].

Aiming at achieving better quality of a grafting procedure, new product formulations were proposed using melt-quenched BG1d-BG powder and organic carriers (*e.g.* glycerol and polyethylene glycol) that appeared in the form of moldable pastes and demonstrated cohesive injectability [26].

This work provides an overview of the synthesis and properties of BG1d-BG powder, preparation of BG1d-BG-glycerol pastes, apatite-forming ability in SBF solution, viscoelastic behavior and structural features revealed by means of scanning electron microscopy (SEM), FTIR and Raman spectroscopy. Furthermore, this study discusses the results of preliminary *In vivo* animal tests conducted through injecting moldable BG1d-BG-based paste into osseous defects made in rabbit's femur.

2 Materials and methods

2.1 Materials preparation

As it has been described elsewhere [24, 27], BG1d-BG was prepared by the melt-quenching technique from powders of technical-grade silicon oxide (purity 99.5%) and calcium carbonate (99.5%), as well as reagent-grade $MgCO_3$, Na_2CO_3, CaF_2, and $NH_4H_2PO_4$ (Sigma-Aldrich, St. Louis, MO, USA). The raw precursors were homogeneously mixed, preheated at 1000°C for 1 h for decarbonization and then melted in platinum crucible at 1400°C for 1 h in air. Glasses in bulk form were produced by pouring the melts on preheated bronze molds followed by annealing at 600°C for 1 h, while glass frits were obtained by quenching of molten glass in cold water. The frit was dried, crushed and milled to get fine powders with mean particle sizes within the range of 10–15 μm (as determined by the light scattering technique; Coulter LS 230, UK, Fraunhofer optical model).

In order to prepare the BG1d-BG-glycerol paste samples (further denoted as BG-gly), glycerol (88 wt.% aqueous solution) with a density of 1.230 g/cm^3 for analysis (Fluka) was manually mixed with the glass powder using metallic spatula until a visual cohesive (homogeneous) distribution of particles throughout glycerol was attained. Particle to carrier ratio was fixed as 73/27 by weight (or 54/46 by volume). Pastes were easily transferred and stored into standard syringes.

2.2 Materials characterization

The apatite-forming ability of BG1d-BG and BG-gly paste were investigated upon immersion in simulated body fluid (SBF) at 37°C keeping the sample-to-SBF ratio as 2 mg/mL. The SBF solution had composition nearly equivalent to that of human plasma, as discussed by Tas [28] (Na^+ 142.0, K^+ 5.0, Ca^{2+} 2.5, Mg^{2+} 1.5, Cl^- 147.8, $(HPO_4)^{2-}$ 1.0, $(HCO_3)^-$ 4.2 and $(SO_4)^{2-}$ 0.5 mmol L^{-1}). The SBF mixtures were sealed immediately after preparation into sterilized plastic flasks and were placed in a dynamic incubator at 37°C (±0.5°C), which was subjected to orbital shaking at 120 rpm. The experiments were performed in duplicate in order to ensure the accuracy of results. After each experiment, the solid particles separated from the liquid were subjected to X-ray diffraction (XRD) measurements performed with a conventional Bragg-Brentano diffractometer (XRD; 2θ = 20–40° with a 2θ-step rate of 0.02°/s; Rigaku Geigerflex D/Mac, C Series, Cu-Kα radiation, Japan).

Microstructure observations were done by field emission scanning electron microscopy (JSM-7600F, JEOL, Akishima shi, Japan).

FTIR spectra were collected by a VARIAN 670IR spectrophotometer using attenuated total reflection (ATR) mode.

2.3 *In vivo* animal tests

In vivo biocompatibility tests were performed with BG-gly pastes. The implantation and histological analyses of the bones with the implants were performed at the Interinstitutional research center, Tashkent Medical Academy, Uzbekistan and at the Faculty of Prosthetic Dentistry, Tashkent State Dental Institute, Uzbekistan. Twenty healthy and completely matured (1-year old) rabbits from the breed "shinshilla" weighing 2.8–3.0 kg were used.

Animals were kept in individual cages, properly identified according to the period and group. Surgery was conducted under applying systemic anesthesia. After being sterilized by gamma irradiation (25kGy), BG-gly paste was injected by syringe into the femoral diaphysis region to fill a previously drilled hole of 2 mm diameter and about 10 mm length. The incised hole was subsequently sewed up. Incision without any implantation with drilling a hole of 2 mm diameter and about 10 mm length was also performed as control.

All surgical procedures were conducted with the permission of the local ethics committee (the Ethical Committee of Uzbekistan under reference no. 9, dated 3.12.2019) and Ministry of Health of Uzbekistan (the certificate issued to the Interinstitutional research center, Tashkent Medical Academy, Uzbekistan under reference no. 3, dated 13.01.2020).

The animals were segmented into 2 groups (control and experimental) and the experiment was divided into three stages of observation of 1, 2 and 3 months according to the Table 1.

After implantation, the rabbits were sacrificed by immediate decapitation. The surgeries and animal care were undertaken in accordance with ethical guidelines and rules of local Governmental bodies. All femurs were subsequently fixed in 10% phosphate buffered formalin for 72 h for histological or histomorphometrical analysis. These femurs were decalcified in 10% formic acid formalin solution for 14 days. The femurs were sectioned parallel to the long axis of the femur through the anteromedial aspect of the defect. The tissue blocks were sectioned and stained with hematoxilin and eosin (H&E) and histopathologically observed by optical microscopy.

The following histological scoring scale for the presence and intensity of bone formation was used for statistical analysis [29, 30]: 1. no osteogenesis, 2. weak osteogenesis, 3. medium-low osteogenesis, 4 medium-high osteogenesis, 5. good-low osteogenesis, 6. good-high osteogenesis, 7. perfect osteogenesis. For this purpose, each slide of histopathological sections was divided into four segments to be observed in detail while the average of the scores of the four quadrants represents the score given to the slide [29].

Since there were two groups - one was the control and the other was the experimental one treated with BG-gly paste, statistical analysis was performed by using Wilcoxon-Mann-Whitney test [29]. The tests were performed with a level of significance of 5%. The test involves the calculation of a statistic, usually called U, whose distribution under the null hypothesis is known [31].

3 Results and discussion

3.1 Properties, structural features and bioactivity of BG1d-BG and BG-gly pastes

Bulk BG1d-BG after melting at 1400°C for 1 h is transparent and colourless material with no crystalline inclusions, as also confirmed by X-ray and SEM analyses afterwards. Properties of BG1d-BG glass are presented in the Table 2.

The microstructure of the annealed BG1d-BG bulk glass (Figure 1) exhibited a liquid-liquid phase separation with droplets of segregated phases composed, according to [32], of silicate and phosphate networks.

Table 1: Protocol of implantation procedure

Observation stage	Empty hall (control)	BG-gly implantation (experimental)
1 month	3 animals per group with numbering in the range No. 1-3	3 animals per group with numbering in the range No. 4-6
2 months	3 animals per group with numbering in the range No. 7-9	3 animals per group with numbering in the range No. 10-12
3 months	4 animals per group with numbering in the range No. 13-16	4 animals per group with numbering in the range No. 17-20

Table 2: Properties of BG1d-BG glass

Bulk density, kg/m^3	2.84 ±0.01
Molar volume, cm^3/mol	20.85 ± 0.07
Glass transition temperature obtained by dilatometry, T_g (°C)	607 ± 7
Peak temperature of crystallization, T_p (°C)	815 ± 13
Coefficient of thermal expansion, CTE	10.6 ± 0.1 × 10^{-6} K^{-1}
Activation energy of crystallization, E_a (kJ/mol)	430 ± 30

Note: Data on density, molar volume and coefficient of thermal expansion were taken from the ref. [33], glass transition temperature peak temperature of crystallization, activation energy of crystallization are from the ref. [34]

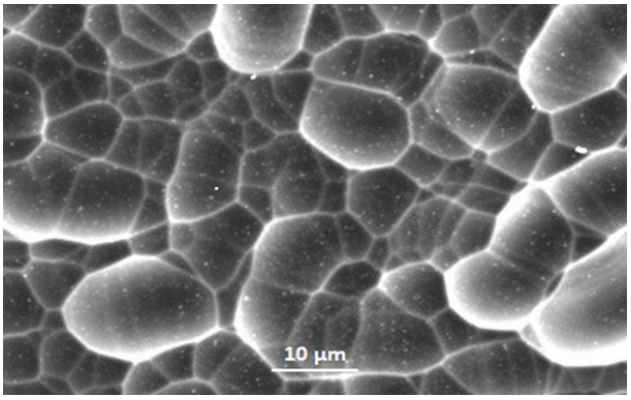

Figure 1: SEM micrograph of the microstructure of the annealed BG1d-BG bulk glass, which revealed liquid-liquid phase separation with droplets of segregated liquid phases

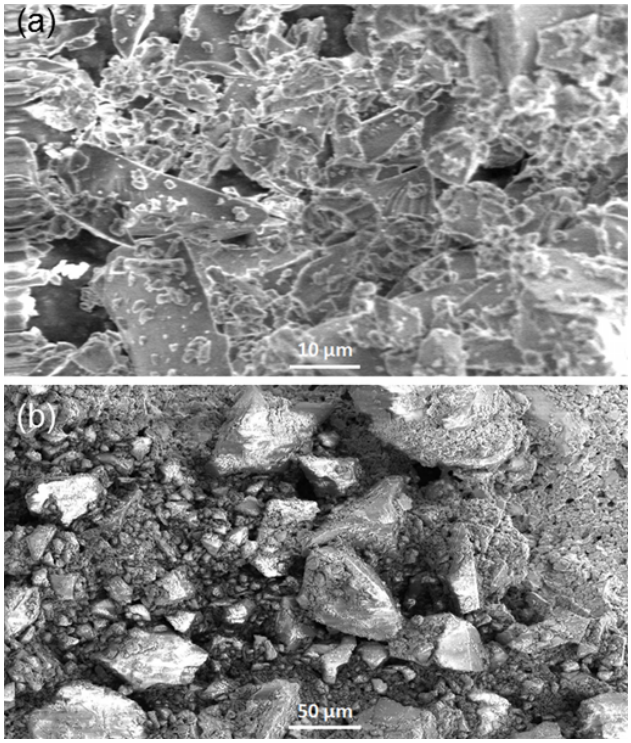

Figure 2: Glass particle morphology: (a) SEM image of BG1d-BG powder and (b) SEM image of as-prepared BG-gly paste

Figure 2a shows a SEM image of glass powder obtained after frit milling, which is composed by agglomeration of particles with irregular and mostly angular shapes featuring aspect ratios ranging from 1 to 2.5. Conversely, the microstructure of BG-gly paste (Figure 2b) shows streamlined glass particles where glycerol spreads well over their surface forming slippery layers and conferring cohesiveness (homogeneousness) to the system [27].

It is well documented that the structure of bioactive glasses defines their dissolution behavior that is in turn controlled by formation of non-bridging oxygen groups (NBOs). For instance, 45S5 glass contains more than two-third non-bridging oxygen atoms per tetrahedron, thus suggesting a high disruption of the glass network [32]. According to FTIR transmittance spectrum (Figure 3a), the experimental BG1d-BG glass exhibited a wide distribution of Q^n (here "n" denotes the number of bridging oxygens, BOs) species, thus suggesting disorder in the silicate and phosphate network [33]: this is witnessed by a lack of sharp features with three broad transmittance bands in the region of 600–1500 cm^{-1}. In particular, the band around 1040 cm^{-1} is attributed to both asymmetric stretch vibration of Si-O$^-$ bonds in silicate Q^3 tetrahedral units [33, 35, 36] and to analogous vibrations of phosphate tetrahedral units (PO_4^{3-}) with 4 NBOs (Q^0 units) [36]. The most intense transmittance band at 926 cm^{-1} might be assigned to asymmetric stretch vibration in silica tetrahedral unit with two and one bridging oxygens since from earlier studies the bands near 950 cm^{-1} and 900 cm^{-1} were attributed to Q^2 and Q^1 units, respectively [37, 38]. This spectrum also shows a broad band at about 755 cm^{-1}, which corresponded to the rocking motion of Si-O-Si bridges with 3 NBOs (Q^1 units).

Figure 3b presents FTIR spectrum of glycerol with two characteristic bands at 1112 and 1038 cm^{-1} assigned to C=OH stretching vibrations [26, 39]. In turn, the FTIR spectrum of BG-gly paste (Figure 3c) exhibited transmittance bands at 1104 and 1027 cm^{-1} which could be attributed to stretching vibrations of C–O–R units [26, 40] and, according to Gonzalo *et al.* [26], it is an indication that glycerol chemically bonds to the surface of the BG1d-BG glass particles. An appearance of the low frequency transmittance band at 675 cm^{-1} might serve as an additional evidence to this assumption.

Analysis of Raman spectra (not shown) of BG1d-BG glass and BG-gly pastes [26] is presented in Table 3.

Table 3: General assignment of Raman bands

Band (cm^{-1})	Assignment	Band intensity
BG1d-BG glass		
ca. 1050	Si-O^- stretching in silicate Q^3 tetrahedral units	very weak
ca. 950	Si-O^- stretching in silicate Q^2 tetrahedral units	very intense
ca. 875	Si-O^- stretching in silicate Q^1 tetrahedral units	very weak
BG-gly paste		
ca. 1050	Q^3 units	intense
ca. 975	Q^2 units	weak
ca. 925	Q^1 units	intermediate
ca. 850	Q^0 units	very intense
ca. 825	Q^0 units	intermediate

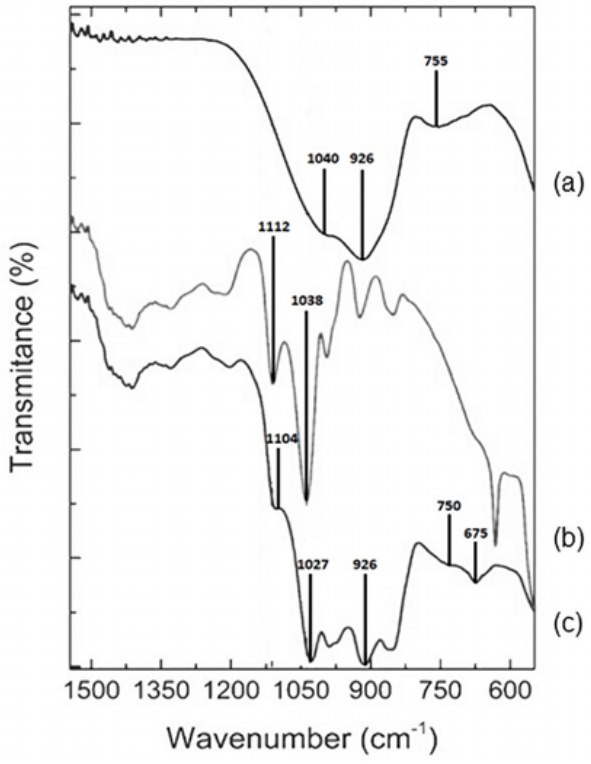

Figure 3: FTIR spectra of (a) as-prepared BG1d-BG, (b) as-received glycerol, (c) as-prepared BG-gly paste

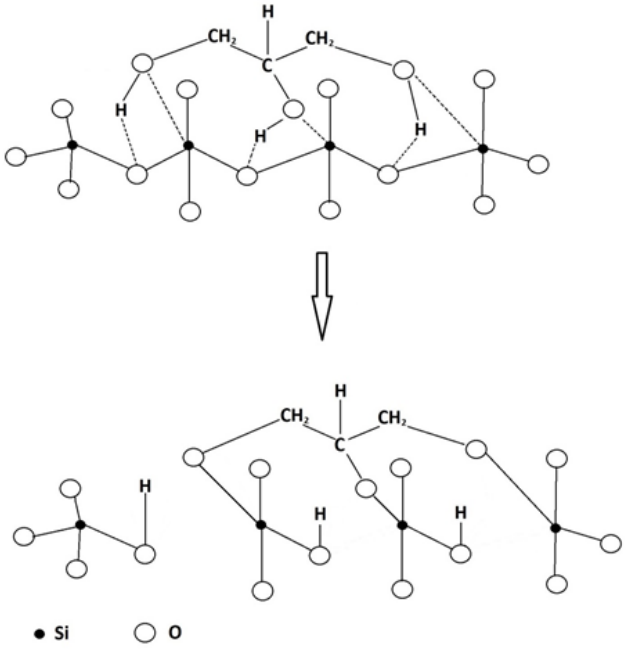

Figure 4: A scheme displaying the chemical interaction between BG1d-BG and glycerol occurred via intermolecular forces (shown as dash lines) upon chemisorption of glycerol molecules on the glass surface. These intermolecular forces caused disrupting of the glass network with formation of silanol groups at the surface, thus favoring apatite formation in physiological solutions

This analysis reveals that Q^2 species (band at ca. 950 cm^{-1}) are dominant structural units in BG1d-BG glass while Q^3 units (band at ca. 1050 cm^{-1}) and Q^1 species (band at ca.875 cm^{-1}) are minor constituents of the network (Table 3).

On the contrary, analysis of Raman bands of BG-gly paste (Table 3) suggests coexistence of Q^3, Q^1 along with newly formed Q^0 units whereas contribution of Q^2 species (*e.g.* weak intensity stretching vibration Si-O^- that occur at ca. 975 cm^{-1}) declined significantly when compared to the original BG1d-BG glass, thereby depicting the chemical change happened between glass and glycerol. Thus, Figure 4 represents a scheme illustrating the feasible interaction occurred via intermolecular forces (shown as dash lines) upon chemisorption of glycerol molecules on the glass surface. This type of chemical interaction ultimately caused disrupting of the glass network with formation of silanol groups at the surface, thus favoring apatite formation in physiological solutions.

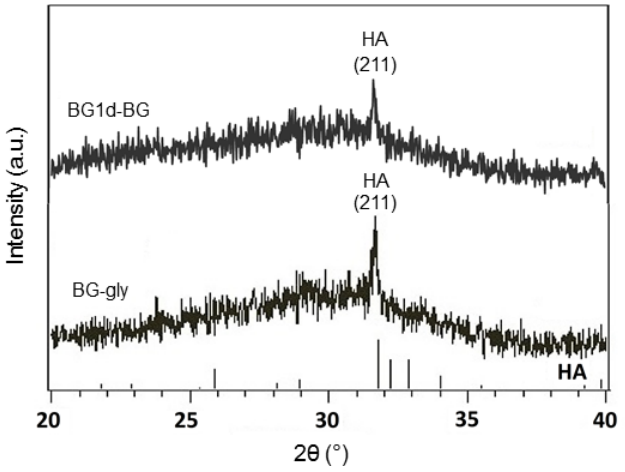

Figure 5: XRD patterns of BG1d-BG and BG-gly after immersion in SBF for 12 h, along with the comparison of diffraction lines for hydroxyapatite (HA)

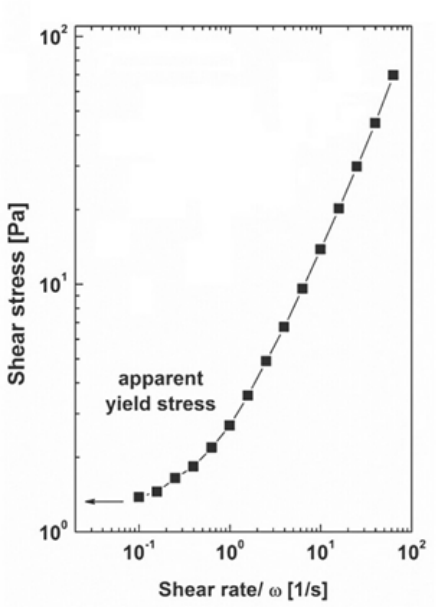

Figure 6: Flow curves of the paste reconstructed from oscillatory tests

XRD patterns of BG1d-BG glass and BG-gly paste after immersion in SBF for 12 h are shown in Figure 5. Although both materials are predominantly amorphous, the main characteristic diffraction peak of hydroxyapatite, appearing at $2\theta = 31.79^\circ$ (reflection (211)), was revealed after a relatively short-time immersion in SBF, thus proving the good bioactive properties of BG1d-BG in the form of both as-such glass and paste. It is worth pointing out that the diffraction peak is slightly sharper and more intense in the case of BG-gly paste. A possible explanation for this fact is that the BG-gly paste featured faster leaching behaviour of Ca^{2+} and Mg^{2+} ions as compared to BG1d-BG glass sample at the initial stages of exposure to SBF (*i.e.* ca. 25 and 50% higher concentrations, respectively, after 3 h immersion in SBF [40]). The enhanced dissolution of $Ca^{2+}$and Mg^{2+} is governed by surface chemistry and is due to significant fraction of Q^1 and Q^0 units in the BG-gly material (Table 3). Moreover, it was well documented in the literature that the most crucial step of the bioactive process is the formation of non-bridging oxygen groups, which controls the dissolution of the silica through formation of silanol groups at the glass surface [2, 3, 5, 32]. Therefore, due to improved biodegradability and faster apatite-forming ability in vitro, BG-gly material might possess advantages for specific applications such as treatment of periodontal diseases [24].

Viscoelastic behavior of pastes is determined by a number of factors where the most critical ones are particle size, size distribution, particle shape, surface morphology and the specific interactions between the solvent molecules and dissolved species [41, 42]. Preliminary injectability tests performed in the earlier study [27] demonstrated that BG-gly pastes with solid loading less than 75 wt.% (*i.e.* 56.5 vol.%) are practically 100% injectable and could be fully extruded: these pastes, after the transient pseudo-plastic flow behavior, enter a Newtonian regime that lasts up to around the end of the extrusion process. It was underlined that the specific interactions between the molecules of the carrying liquids and the surface of BG particles exert a great influence on the maximum achievable solid loading and on flow behaviour of the resulting pastes. As for composition under test (73 wt.% glass to 27 wt.% glycerol ratio or 54 vol.% glass to 46 vol.% glycerol ratio), the flow curves reconstructed from oscillatory tests [26] exhibited apparent yield stress values at low shear rate/frequency (Figure 6). This paste shows pseudoplastic behaviour expressed by the faster increasing trends of shear stress with increasing deformation rate at low and medium values. This means that there is room for further improving the flow behaviour of the pastes by suitably adjusting the experimental parameters that play key roles in determining their rheological behaviour [26, 27]. In general, the carrier to be added to bone graft formulation must be carefully selected [43]: it should be biocompatible, its major amount should be cleared away fast enough to allow bone formation on the surface of the bone graft, it should optimize the handling characteristic of the bone graft formulation and allow retention of the particles of bone graft in a bony defect. Thus, Davison *et al.* [44] demonstrated that a paste prepared from TCP (50 vol%) and organic carrier (50 vol%) (where carrier composition was 5 wt.% carboxymethyl cellulose and 95 wt/% glycerol) allowed the

in vitro surface mineralization of TCP by day 7 and produced the highest level of orthotopic bone bridging and ectopic bone formation, which was equivalent to the control. Selection of glycerol as organic carrier is based on its documented biocompatibility, water solubility, cohesions when combined with bone graft particles and adhesion to wet bone [43–46].

The chemical degradation tests performed earlier for BG1d-BG and BG-gly paste in Tris-HCl at 37°C in static regime without solution replacement revealed that mass loss after 120 h was 2.81 wt% and 28.46 wt%, respectively [40]. Considering that the BG-gly sample consists of 27 wt% glycerol, one can conclude that relatively fast dissolution of glycerol from glass surface occurs. However, the chemically bonded glycerol may not get released at once while being leached over time, thus providing required initial osteoconductivity to orthotopic sites of implantation and allowing cohesion of the bioactive glass particles to bone defect.

3.2 Animal model

BG–gly materials appeared to be fully injectable into femoral diaphysis region to fill a hole of 2 mm diameter and about 10 mm length. Over the whole implantation period, the rabbits exhibited ordinary behavior with no reports of adverse effects, such as allergies or other immunologic reactions, abscess formation, or rejection of the grafting paste. The following characteristic features were analyzed during the observation of tissue blocks under optical microscopy: (a) the presence of inflammatory infiltrate, (b) the woven bone formation in the margins of the wound, (c) the woven bone formation in the center of the wound and (d) transformation of woven bone to laminar bone. Figure 7 shows that, after 1 month post-implantation, no inflammatory infiltrate was present either in the experimental or in the control group, unlike what was usually observed in the literature (formation of inflammatory infiltrate not later than 2-3 weeks [27, 46]). In the center of the Figure 7a, direct splicing of non-resorbed glass particulates (denoted as **BG** for the sake of simplicity) with bone trabeculae is clearly seen after 1 month of implantation, thus confirming the bone-bonding ability of BG1d-BG bioactive glass. Moreover, numerous osteocytes in the form of white spots can be easily revealed within the area occupied by glass residues, thus suggesting the gradual resorption of glass followed by ossification. Generally, after one month of implantation, formation of new bone was more advanced in the experimental group (Table 4) compared to the control group (Figure 7b) due to weak osteogenesis of the latter with presence of loose connective tissue in the area of the defect, incomplete filling of the cavity and rarefaction. Importantly, in the experimental group, bone repair in the form of woven bone appears in intimate contact with bone graft surface; this is consistent with previous observations by other authors who investigated different bioactive glass compositions [46–48]. After 2 months, further resorption of the bioactive material followed by osteointegration can be observed (Figure 7c). In particular, woven bone (*e.g.* part of the region denoted as 4, Figure 7c) was gradually substituted by lamellar one (*e.g.* region denoted as 1, Figure 7c) in the margins of bone graft due its resorption.

Unlike the experimental group, the control group defect was still filled with loose connective tissue and demonstrated incomplete compaction (Figure 7d, Table 4). In the experimental group after 3 months of implantation, residues of glass were completely embedded into bone trabeculae suggesting full resorption of bone graft. In the Figure 7e, compact laminar tissue that was formed at the expense of bone graft demonstrated high level of osteointegration (region denoted as 1) to old bone (region denoted as 3). At the right side of Figure 7e, (region denoted as 2) fragmentation of cavities by trabeculae with elements of yellow bone marrow is seen, demonstrating different steps of bone remodeling in the areas close to implantation site. In control group, histology after 3 months of implantation (Figure 7f) demonstrates immature connective tissue in the defect area (region denoted as 5), thus suggesting delayed regeneration compared to the experimental group (Table 4).

Statistical analysis performed using Wilcoxon-Mann-Whitney test showed that calculated U values (data for calculation are shown in Table 4) were either equal or lower than critical tabulated U value, *i.e.* U calculated ≤ U criti-

Table 4: Bone formation score for control and experimental groups according to data of Table 1 and histological scoring scale

Observation stage	Empty hall (control)	BG-gly implantation (experimental)
1 month	No. 1 / score 2	No. 4 / score 4
	No. 2 / score 2	No. 5 / score 4
	No. 3 / score 2	No. 6 / score 4
2 months	No. 7 / score 3	No. 10 / score 5
	No. 8 / score 2	No. 11 / score 6
	No. 9 / score 3	No. 12 / score 5
3 months	No. 13 / score 4	No. 17 / score 6
	No. 14 / score 3	No. 18 / score 6
	No. 15 / score 4	No. 19 / score 7
	No. 16 / score 3	No. 20 / score 5

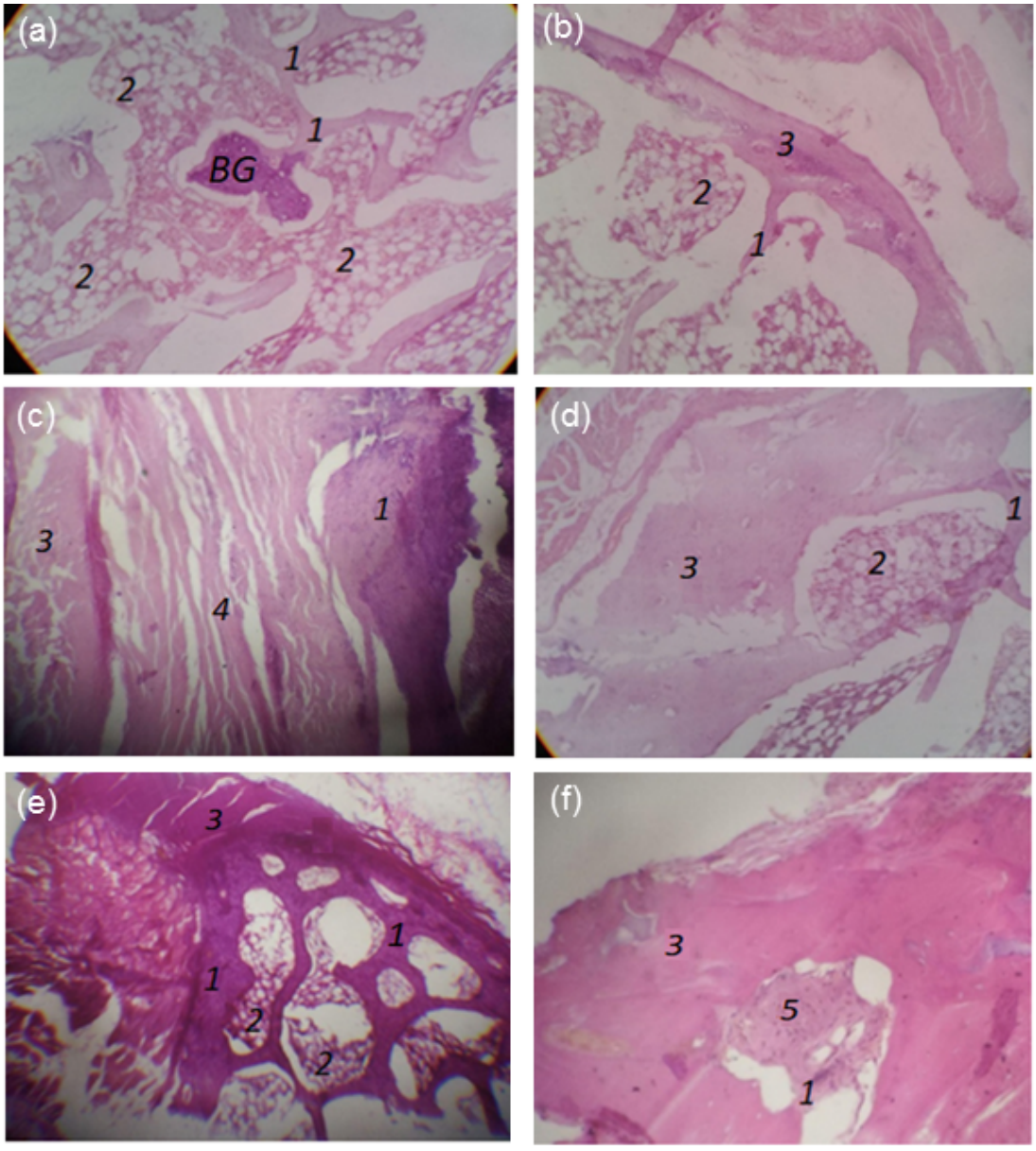

Legend: BG – residue of bone graft with embedded osteocytes (experimental group after one month), 1-New bone, 2-Yellow bone marrow, 3-Old bone, 4-Fibrous osteogenic tissue/woven bone, 5 -Fibroreticular tissue of osteogenic structure

Figure 7: Histopathological sections in cortical area of bone after different periods of paste implantation: (A) experimental group (BG-gly) after 1 month (original magnification 10.0×), (B) control group after 1 month (original magnification 4.0×), (C) experimental group after 2 months (original magnification 10.0×), (D) control group after 2 months (original magnification 10.0×), (E) experimental group after 3 months (original magnification 10.0×), and (F) control group after 3 months (original magnification 10.0×)

cal always. This means that there is significant difference between intensity of bone formation score in the control and the experimental groups at all 3 tested periods of implantation. Thus, the "osteogenetic effect" is statistically significant, suggesting that this effect is real and is not due to chance. Further experimentation of longer implantation period is currently underway to get deeper inside of influence of BG-gly paste on bone healing and remodelling.

It is well documented that fracture healing, being a complex biological process, normally includes acute inflammatory response, recruitment of mesenchymal stem cells (MSCs), generation of cartilaginous bony callus, mineralization, revascularization, and resorption of cartilaginous callus, and finally bone remodeling [49, 50]. Shapiro and Wu, [50] revealed that as soon as a drilling defect through one cortex of the diaphysis of a young rabbit fe-

mur was made, blood filled the space and fibrinous arcades formed within the blood clot across the defect from wall to wall; undifferentiated mesenchymal cells lay parallel to the fibrinous arcade, in conjunction with vascularization. The transformation from undifferentiated mesenchymal cells to a mesenchymal osteoblast, with increasing woven tissue synthesis, to a surface osteoblast synthesizing lamellar on woven bone, was found. New bone formation beginning in the marrow advanced to the periphery of the defect while repair did not occur uniformly with the same tissue pattern across the entire defect and the central defect region healing last [50]. The woven bone is then remodeled into lamellar bone over the course of months to years, which allows for restoration of the canal and its bony properties [50].

It is worth pointing out that an ideal bone grafting material should safely dissolve once it has performed its function in the body, thus being then fully replaced by new healthy tissue. This condition can be achieved when phosphate glasses are used [51, 52], but it is much more difficult to fulfil if silicate bioactive glasses are used. 45S5 glass particles were shown to persist after 12 post-operative weeks in a rabbit femur after being embedded in new bone [53]. In the same study, the resorption rate of sol-gel 77S and 58S bioactive glass particles was found to be greater than that of melt-derived 45S5 particles but full resorption was not achieved. Heikkila *et al.* reported that some particles of S53P4 glass (marketed under the tradename of BonAlive®) were still present after 11 years post-implantation [54]. The lack of full resorption of S53P4 glass may be due to glass composition, which has higher silica content than 45S5 (53 vs. 45 wt.%). BG1d-BG has a silica content (46.1 wt.%) close to that of 45S5 glass, which could explain its high tendency to resorb *In vivo*.

4 Conclusions

BG-gly paste shows an improved bioactivity as compared to the neat BG1d-BG glass that relies on chemical interaction of glycerol with the surface of the glass. This results in a strong decrease of the network connectivity of bioactive glass as well as a significant increase of the amount of surface silanol groups. Being practically 100% injectable, the prepared BG-gly paste shows promise in fulfilling a couple of key "technical" requirements for being a bone regeneration material, *i.e.* (i) the ease of use by the surgeon and (ii) the ability to conform to the geometry of the osseous defect. Preliminary *In vivo* animal tests demonstrated that BG-gly paste is a biocompatible material able to promote bone regeneration. It was demonstrated that there is a statistically significant difference between the intensity of bone formation score in the control and the experimental groups at all 3 tested periods of implantation. Glass particulate from BG-gly paste elicited an osteogenetic effect and was prone to completely resorb within 3 months post-implantation while woven bone was gradually substituted by lamellar one, which suggests its potential application in osteostimulatory bone healing.

Acknowledgement: D.U.T. acknowledges financial support from Alexander von Humboldt Foundation (Project "Development and characterization of new family polymer –derived glasses and glass-organic composites with high bioactivity for bone tissue repair"). D.U.T. thanks Dr. I. Gonzalo-Juan and Dr. E. Ionescu from the Technical University Darmstadt (Germany), Prof. J.M.F. Ferreira from the University of Aveiro (Portugal), and Prof. C. Balan from the Politehnica University Bucharest (Romania) for their valuable help in discussion of the obtained results.

Ethical approval: The research related to animals' use has been complied with all the relevant national regulations and institutional policies for the care and use of animals.

Conflict of Interests: The authors declare no conflict of interest regarding the publication of this paper.

References

[1] Jones J.R., Brauer D.S., Hupa L., Greenspan D., Bioglass and bioactive glasses and their impact on healthcare, Int. J. Appl. Glass Sci., 2016, 7, 423-434.
[2] Fernandes H.R., Gaddam A., Rebelo A., Brazete D., Stan G.E., Ferreira J.M.F., bioactive glasses and glass-ceramics for healthcare applications in bone regeneration and tissue engineering, Materials, 2018, 11, 2530.
[3] Hench L.L., Bioceramics - from concept to clinic, J. Am. Ceram. Soc., 1991, 74, 1487-1510.
[4] Hench L.L., The story of Bioglass®, J. Mater. Sci. Mater. Med., 2006, 17, 967-978.
[5] Fiume E., Barberi J., Verné E., Baino F., Bioactive glasses: from parent 45s5 composition to scaffold-assisted tissue-healing therapies, J. Funct. Biomater., 2018, 9, 24.
[6] Baino F., Hamzehlou S., Kargozar S., Bioactive glasses: where are we and where are we going? J. Funct. Biomater., 2018, 9, 25.
[7] Fagerlund S., Understanding the in vitro dissolution rate of glasses with respect to future clinical applications, department of chemical engineering, Åbo Akademi Process Chemistry Centre, Laboratory of Inorganic Chemistry, Åbo Akademi University, Turku, 2012.
[8] Hench, L.L., Genetic design of bioactive glass, J. Eur. Ceram. Soc., 2009, 29, 1257-1265.

[9] Hench L.L., Hench J.W., Greenspan D., Bioglass: a short history and bibliography, J. Australas. Ceram. Soc. 2004, 40, 1-42.
[10] Zamet J., Darbar U., Griffiths G., Bulman J., Brägger U., Bürgin W., Newman H., Particulate Bioglass® as a grafting material in the treatment of periodontal intrabony defects, J. Clin. Periodontol., 1997, 24, 410-418.
[11] Profeta A.C., Huppa C., Bioactive glass in oral and maxillofacial surgery, Craniomaxillofac. Trauma Reconstr., 2016, 9, 1-14.
[12] Skallevold H.E., Rokaya D., Khurshid Z., Zafar M.S., Bioactive glass applications in dentistry, Int. J. Mol. Sci., 2019, 20, 5960.
[13] Tadjoedin E.S., De Lange G.L., Lyaruu D., Kuiper L., Burger, E.H., High concentrations of bioactive glass material (Biogran®) vs. autogenous bone for sinus floor elevation, Clin. Oral Implants Res., 2002, 13, 428-436.
[14] Ashman A., Gross J.S., Synthetic osseous grafting. In: Wise D.L., Trantolo D.J., Lewandrowski KU., Gresser J.D., Cattaneo M.V., Yaszemski M.J. (eds) Biomaterials Engineering and Devices: Human Applications. Humana Press, Totowa, NJ, 2000, pp. 133-154.
[15] Profeta, A.C., Prucher G.M., Bioactive glass in periodontal surgery and implant dentistry, Dent. Mater. J., 2015, 34, 559-571.
[16] Sohrabi K., Saraiya V., Laage T.A., Harris M., Blieden M., Karimbux N., An evaluation of bioactive glass in the treatment of periodontal defects: a meta-analysis of randomized controlled clinical trials, J. Periodontol., 2012, 83, 453-464.
[17] Subbaiah R., Thomas B., Efficacy of a bioactive alloplast, in the treatment of human periodontal osseous defects-a clinical study, Med. Oral Patol. Oral Cirugia Bucal, 2011, 16, e239-244.
[18] Park J.S., Suh J.J., Choi S.H., Moon I.S., Cho K.S., Kim C.K., Chai J.K., Effects of pretreatment clinical parameters on bioactive glass implantation in intrabony periodontal defects, J. Periodontol., 2001, 72, 730-740.
[19] Anderegg C.R., Alexander D.C., Freidman M., A bioactive glass particulate in the treatment of molar furcation invasions, J. Periodontol., 1999, 70, 384-387.
[20] Ong M.M., Eber R.M., Korsnes M.I., MacNeil R.L., Glickman G.N., Shyr Y., Wang H.L., Evaluation of a bioactive glass alloplast in treating periodontal intrabony defects, J. Periodontol., 1998, 69, 1346-1354.
[21] Froum S.J., Weinberg M.A., Tarnow D., Comparison of bioactive glass synthetic bone graft particles and open debridement in the treatment of human periodontal defects - a clinical study, J. Periodontol., 1998, 69, 698-709.
[22] Baino F., Bioactive glasses - when glass science and technology meet regenerative medicine, Ceram. Int., 2018, 44, 14953-14966.
[23] Sculean A., Windisch P., Keglevich T., Gera I., Clinical and histologic evaluation of an enamel matrix protein derivative combined with a bioactive glass for the treatment of intrabony periodontal defects in humans, Int. J. Period. Restorative Dent., 2005, 25, 139-147.
[24] Tulyaganov D.U., Makhkamov M.E., Urazbaev A., Goel A., Ferreira J.M.F., Synthesis, processing and characterization of a bioactive glass composition for bone regeneration, Ceram. Int., 2013, 39, 2519-2526.
[25] Schmitz S.I., Widholz B., Essers C., Becker M., Tulyaganov D.U., Moghaddama A., Gonzalo de Juan I., Westhauser F., Superior biocompatibility and comparable osteoinductive properties: sodium-reduced fluoride-containing bioactive glass belonging to the CaO–MgO–SiO_2 system as a promising alternative to 45S5 bioactive glass, Bioactive Mater., 2020, 5, 55-65.
[26] Gonzalo-Juan I., Tulyaganov D.U., Balan C., Linser R., Ferreira J.M.F., Riedel R., Ionescu E., Tailoring the viscoelastic properties of injectable biocomposites: a spectroscopic assessment of the interactions between organic carriers and bioglass particles, Mater. Design, 2016, 97, 45-50.
[27] Tulyaganov D.U., Reddy A.A., Siegel R., Ionescu E., Riedel R., Ferreira J.M.F., Synthesis and in vitro bioactivity assessment of injectable bioglass-organic pastes for bone tissue repair, Ceram. Int., 2015, 41, 9373-9382.
[28] Tas A.G., Synthesis of biomimetic Ca-hydroxyapatite powders at 37°C in synthetic body fluids, Biomaterials, 2000, 21, 1429-1438.
[29] Camargo A.F.F., Baptista A.M., Natalino R., Camargo O.P., Bioactive glass in cavitary bone defects: a comparative experimental study in rabbits, Acta Ortop. Bras., 2015, 23, 202-207.
[30] Bellucci D., Cannillo V., Anesi A., Salvatori R., Chiarini L., Manfredini T., Zaffe D., Bone Regeneration by novel bioactive glasses containing strontium and/or magnesium: a preliminary in-vivo study, Materials, 2018, 11, 2223.
[31] Kharkova A., Grjibovski A.M., Analysis of two independent samples using stata software: non parametric criteria, Ekologiya Cheloveka (Human Ecology), 2014, 4, 60-63. [in Russian].
[32] Tilocca A, Structural models of bioactive glasses from molecular dynamics simulations, Proc. R. Soc. A, 2009, 465, 1003-1027.
[33] Kansal I., Tulyaganov D.U., Goel A., Pascual M.J., Ferreira J.M.F., Structural analysis and thermal behavior of diopside-fluorapatite-wollastonite glasses and glass-ceramics, Acta Biomater., 2010, 6, 4380-4388.
[34] Dimitriadis K., Moschovas D., Tulyaganov D.U., Agathopoulos S., development of novel bioactive glass-ceramics in the Na_2O/K_2O-CaO-MgO-SiO_2-P_2O_5-CaF_2 system, J. Non-Cryst. Solids, 2020, 533, 119936.
[35] Stoch L., Sroda M., Infrared spectroscopy in the investigation of oxide glasses structure, J. Mol. Struct., 1999, 511-512, 77-84.
[36] Agathopoulos S., Tulyaganov D.U., Ventura J.M.G., Kannan S., Saranti A., Karakassides M.A., *et al.* Structural analysis and devitrification of glasses based on the CaO–MgO–SiO_2 system with B_2O_3, Na_2O, CaF_2 and P_2O_5 additives, J. Non-Cryst. Solids, 2006, 352, 322-328.
[37] Merzbacher C.I., White W.B., Structure of Na in aluminosilicate glasses – a far-infrared reflectance spectroscopic study, Am. Mineral., 1988, 73, 1089-1094.
[38] Furukawa T., Brawer S.A., White W.B., The structure of lead silicate glasses determined by vibrational spectroscopy, J. Mater. Sci., 1978, 13, 268-282.
[39] Hidawati E.N., Sakinah A.M.M., Treatment of glycerin pitch from biodiesel production, Int. J. Chem. Environ. Eng., 2011, 2, 309-313.
[40] Tulyaganov D., Abdukayumov K., Ruzimuradov O., Hojamberdiev M., Ionescu E., Riedel R., Effect of alumina incorporation on the surface mineralization and degradation of a bioactive glass (CaO-MgO-SiO_2-Na_2O-P_2O_5-CaF_2)-glycerol paste, Materials, 2017, 10, 1324.
[41] Olhero S.M., Ferreira J.M.F., Particle segregation phenomena occurring during the slip casting process, Ceram. Int., 2002, 28, 377-386.
[42] Olhero S.M., Ferreira J.M.F., Influence of particle size distribution on rheology and particle packing of silica-based suspensions, Powder Technol., 2004, 139, 69-75.
[43] Weinzapfel B., Son-Hing J.P., Armstrong D.G., *et al.* Fusion rates after thoracoscopic release and bone graft substitutes in idio-

pathic scoliosis, Spine, 2008, 33, 1079-1083.
[44] Davison N., Yuan H., De Bruijn J.D., Barrere-de Groot F., *In vivo* performance of microstructured calcium phosphate formulated in novel water-free carriers, Acta Biomater., 2012, 8, 2759-2769.
[45] Park H.W., Lee J.K., Moon S.J., Seo S.K., Lee J.H., Kim S.H., The efficacy of the synthetic interbody cage and grafton for anterior cervical fusion. Spine, 2009, 34, E591-595.
[46] Heikkilä J.T., Aho H.J., Yli-Urpo A., Happonen R.P., Aho A.J., Bone formation in rabbit cancellous bone defects filled with bioactive glass granules, Acta Orthop. Scand., 1995, 66, 463
[47] Bellucci D., Cannillo V., Anesi A., Salvatori R., Chiarini L., Manfredini T., Zaffe D., Bone regeneration by novel bioactive glasses containing strontium and/or magnesium: a preliminary in-vivo study, Materials, 2018, 11, 2223.
[48] Crovace M.C., Souza M.T., Chinaglia C.R., Peitl O., Zanotto E.D., Biosilicate® — a multipurpose, highly bioactive glass-ceramic. in vitro, *In vivo* and clinical trials, J. Non-Cryst. Solids 2016, 432, 90-110.
[49] Perez J.P., Kouroupis, D., Li D.J., Best T.M., Kaplan L., Correa D., Tissue engineering and cell-based therapies for fractures and bone defects, Front. Bioeng. Biotechnol., 2018, 6, 105.
[50] Shapiro F., Wu J.Y., Woven bone overview: structural classification based on its integral role in development, repair and pathological bone formation throughout vertebrate groups, Eur. Cells Mater., 2019, 38, 137-167.
[51] Knowles J.C., Phosphate based glasses for biomedical applications, J. Mater. Chem., 2003, 13, 2395-2401.
[52] Abou Neel E.A., Pickup D.M., Valappil S.P., Newport R.J., Knowles J.C., Bioactive functional materials: a perspective on phosphate-based glasses, J. Mater. Chem., 2009, 19, 690-701.
[53] Wheeler, D.L., Eschbach E.J., Hoellrich R.G., Montfort M.J., Chamberland D.L., Assessment of resorbable bioactive material for grafting of critical-size cancellous defects, Orthop. Res., 2000, 18, 140-148.
[54] Heikkila J.T., Kukkonen, J., Aho, A.J., Moisander, S., Kyyronen, T., Mattila, K., Bioactive glass granules: a suitable bone substitute material in the operative treatment of depressed lateral tibial plateau fractures: a prospective, randomized 1 year follow-up study, J. Mater. Sci. Mater. Med., 2011, 22, 1073-1080.